Journal of Coastal Research	22	0	000–000	West Palm Beach, Florida	Month 0000

Morphological and Sedimentological Impacts of Hurricane Ivan and Immediate Poststorm Beach Recovery along the Northwestern Florida Barrier-Island Coasts

Ping Wang, James H. Kirby, Joseph D. Haber, Mark H. Horwitz, Paul O. Knorr, and Jennifer R. Krock

Department of Geology
University of South Florida
4202 E. Fowler Avenue
Tampa, FL 33620, U.S.A.
pwang@chuma1.cas.usf.edu

ABSTRACT

WANG, P.; KIRBY, J.H.; HABER, J.D.; HORWITZ, M.H.; KNORR, P.O., and KROCK, J.R., 2006. Morphological and sedimentological impacts of Hurricane Ivan and immediate poststorm beach recovery along the northwestern Florida barrier-island coasts. *Journal of Coastal Research,* 22(0), 000–000. West Palm Beach (Florida), ISSN 0749-0208.

Ivan, a strong Category 4 hurricane (downgraded to a Category 3 at landfall), caused widespread erosion and overwash along the northwestern Florida barrier-island beaches. This study examines the storm impact and short-term poststorm recovery along a 200-km stretch of coast from Fort Walton Beach eastward to St. George Island. One prestorm and three poststorm beach-profile surveys were conducted to quantify the storm-induced morphological changes and poststorm recovery. Forty-six trenches were excavated to study the characteristics and thickness of subaerial storm deposits.

Extensive inundation and overwash occurred within 100 km from the storm center at landfall. Significant beach/dune erosion was measured as far as 300 km east of the storm center. The highest elevation of beach erosion extended considerably above the measured storm-surge level, indicating that storm-wave setup and swash run-up played significant roles in controlling the elevation of beach erosion. A simple empirical formula reproduced the wave setup and swash run-up reasonably well. Beach recovery began immediately after the storm. Within 90 days, the berm crest recovered to its prestorm elevation, although it was now located approximately 15 m landward for nonoverwashed sites and 30 to 40 m for overwashed sites. The steep prestorm foreshore slope was restored from the gentle storm profile within 30 days.

An apparent erosional surface was observed along the impacted foredune and backbeach, extending over 300 km eastward from the storm center. This erosional surface represents a net elevation loss ranging from 0.5 to over 2.0 m. A storm layer of up to 50 cm thick was deposited above the erosional surface. Generally, the storm-layer thickness decreases away from the storm center, as well as landward from the high tide line. Local factors such as beach width and orientation, and sediment properties and supply caused variations in the thickness of storm deposit.

ADDITIONAL INDEX WORDS: *Hurricanes, beach erosion, coastal morphology, nearshore sediment transport, storm deposits, storm surge, wave setup.*

?1

INTRODUCTION

Hurricane Ivan made landfall along the northwestern Florida and Alabama coast on September 16, 2004. Ivan briefly reached Category 5 strength, and persisted as a strong Category 4 hurricane in the Gulf of Mexico before being downgraded to a strong Category 3 at landfall by the US National Hurricane Center. Ivan was one of four strong hurricanes that directly impacted Florida coasts within a 1-month period. Apparent and dramatic morphological and sedimentological impacts extend over 300 km eastward from the center of the hurricane.

The Florida panhandle and the general northern Gulf coast are of relatively low wave and tide energy. Less than 10% of the waves measured in a 4-year period at East Pass near the west end of the study area are higher than 1.0 m (MORANG, 1992). Wave periods are typically shorter than 6.0 seconds. Tides are primarily diurnal, with a range typically less than 0.5 m (MORANG, 1992).

Storm impact along barrier island coasts has been the subject of numerous studies (*e.g.,* FINKL and PILKEY, 1991; STONE and FINKL, 1995; STONE and ORFORD, 2004). Because of the largely unpredictable nature of extreme storms like hurricanes, most studies concentrate on poststorm impact and behavior, whereas systematic collection of prestorm data is typically not conducted. This lack of prestorm data makes it difficult to quantify the dramatic morphological impact of storms as well as poststorm recovery.

The impact of a storm on a barrier island is dependent on both the magnitude of the storm-forced parameters, such as storm surge and high waves, and the morphological characteristics of the barrier island, especially the vertical dimension (MORTON and SALLENGER, 2003; SALLENGER, 2000). SALLENGER (2000) developed an impact scale incorporating both storm and morphological parameters. Four parameters, D_{HIGH}, D_{LOW}, R_{HIGH}, and R_{LOW}, are used to evaluate the level

DOI:10.2112/05–0440.1 received 12 May 2005; accepted in revision 17 June 2005.

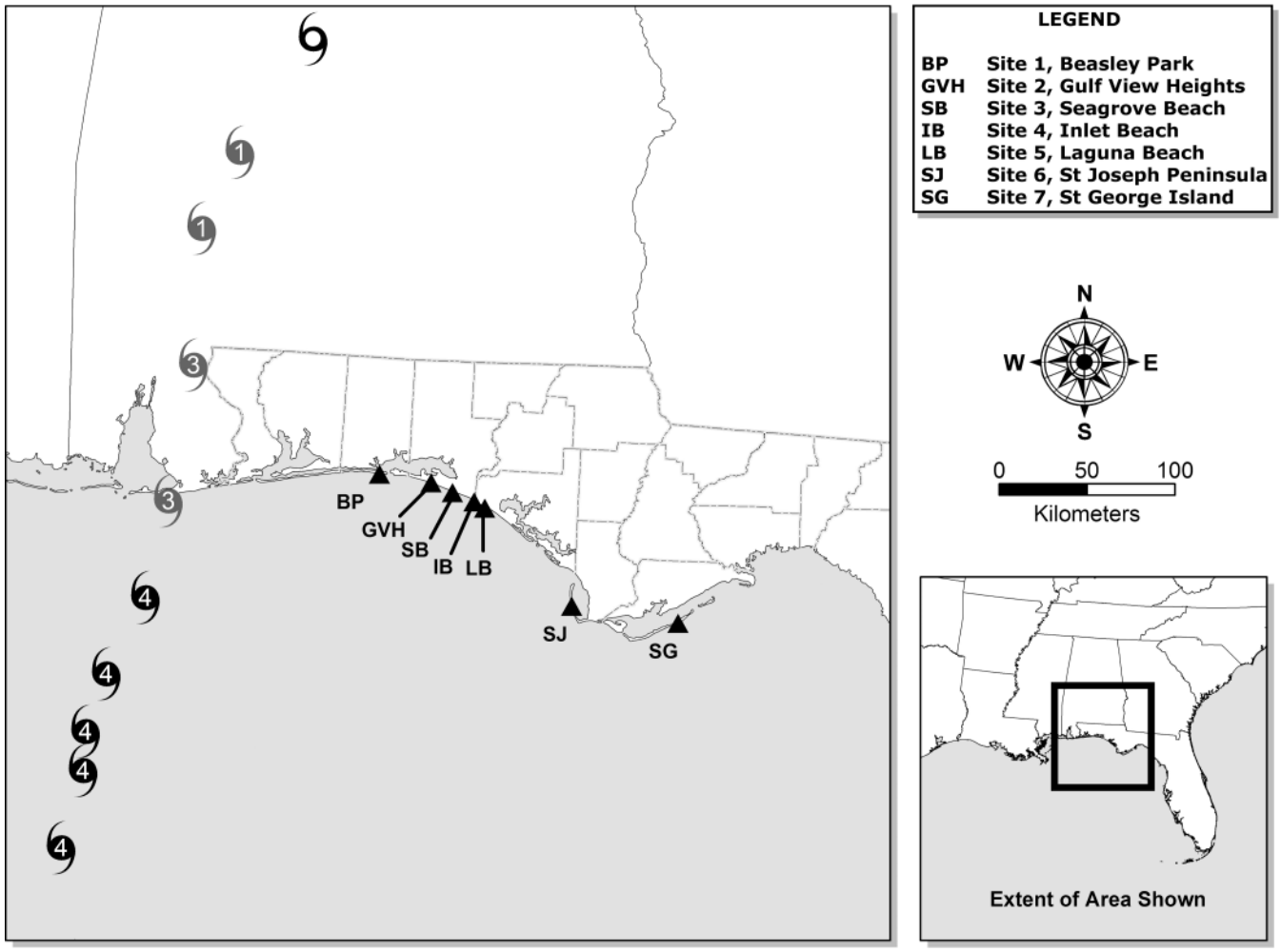

Figure 1. Track and intensity of Hurricane Ivan and locations of the seven study sites.

of morphological impact of storms. D_{HIGH} is the elevation of the highest part of the "first line of defense" (*e.g.,* the foredune ridge). D_{LOW} is the elevation of the base of the dune for beaches with a foredune ridge. For beaches without a foredune ridge, $D_{LOW} = D_{HIGH}$. R_{HIGH} and R_{LOW} are representative high and low elevations of the landward margin of swash. When R_{HIGH} is lower than D_{LOW}, *swash regime,* the first and least severe impact level, occurs. When R_{HIGH} is lower than D_{HIGH} but higher than D_{LOW} (on beaches with a foredune ridge), *collision regime,* the second impact level, occurs. Dune scarping is a typical response under collision regime and is commonly observed after storm impact (*e.g.,* FITZGERALD, VAN HETEREN, and MONTELLO, 1994; TEDESCO *et al.,* 1995; WELLS and MCNINCH, 1991). Using high-resolution ground-penetrating radar, DOUGHERTY, FITZGERALD, and BUYNEVICH (2004) and BUYNEVICH, FITZGERALD, and VAN HETEREN (2004) identified preserved dune scarps in the subsurface strata. When R_{HIGH} is higher than D_{HIGH} but R_{LOW} is lower than D_{HIGH}, *overwash regime,* the third impact scale, occurs (MORTON and SALLENGER, 2003). The fourth and most severe impact, *inundation regime,* occurs when R_{LOW} exceeds D_{HIGH}. Low-lying barrier islands are especially susceptible to inundation regime (DINGLER and REISS, 1995).

In this study, both the dramatic erosion and the deposition induced by Hurricane Ivan are investigated. Three cross-barrier-island profiles and seven beach/dune profiles along the northwestern Florida panhandle coast were surveyed 1.5 days before the hurricane landfall, and 1 week, 4 weeks, and 11 weeks after. The study area extends from Fort Walton Beach, approximately 120 km east of the hurricane center at landfall, to St. George Island, about 300 km east (Figure 1). The goal of the morphological study is to quantify the magnitude of hurricane impact and immediate posthurricane recovery over a large area.

This study also examined the characteristics and thickness of the subaerial storm deposits in 46 trenches excavated along the entire study area (Figure 1). The goal of the sedimentological study is to quantify the characteristics and trends of subaerial storm deposits relative to the distance from the storm center, in addition to the variations across

shore. The depositional effects of significant hurricanes are often overshadowed by the dramatic erosional impacts.

STUDY AREA

The study area extends along the eastern side (with onshore wind) of the hurricane from Fort Walton Beach to St. George Island (Figure 1). Seven study sites along the 200-km stretch of coast were selected. All the study sites are located along the barrier island coast and are composed of dominantly fine to medium quartz sand with variable amounts of heavy minerals (STONE, 1991; USDA-SCS, 1984). For the convenience of discussion, the sites are labeled 1 through 7 from west to east. Site 1, the westernmost site, is located at Beasley Park (referred to as S1_BP in the following) in Fort Walton Beach, approximately 120 km from the center of the storm at landfall. Measuring from the eastern side of the hurricane eyewall at landfall, S1_BP is roughly 80 km to the east. Because of the close proximity to the hurricane center, both significant dune erosion and overwash occurred (Figure 2). The aerial photo in Figure 2 was taken 2 days after the hurricane impact.

Two beach/dune profiles and one cross-island profile were surveyed at the S1_BP site (Figure 2). The first profile, S1_BP1, is located in an area with a relatively high and densely vegetated dune field. The second profile, S1_BP2, is located at the edge of the dune field extending seaward from the top of a high dune. The third profile, S1 BP3, is a cross-island profile and was completely overwashed. This overwash caused severe damage to the four-lane highway (US-98) parallel to the shoreline (Figure 2). The dune at S1_BP2 survived despite the significant erosion of its base, whereas the surrounding area was severely overwashed. No evidence of overwash was noted at S1_BP1. An array of 6 trenches was excavated at S1_BP2 to examine the subaerial storm deposit in front the dune field and on the beach. An array of seven trenches was excavated across the overwash fan at S1_BP3.

The second study site is located at Gulf View Heights (S2_GVH), approximately 150 km east of the storm center at

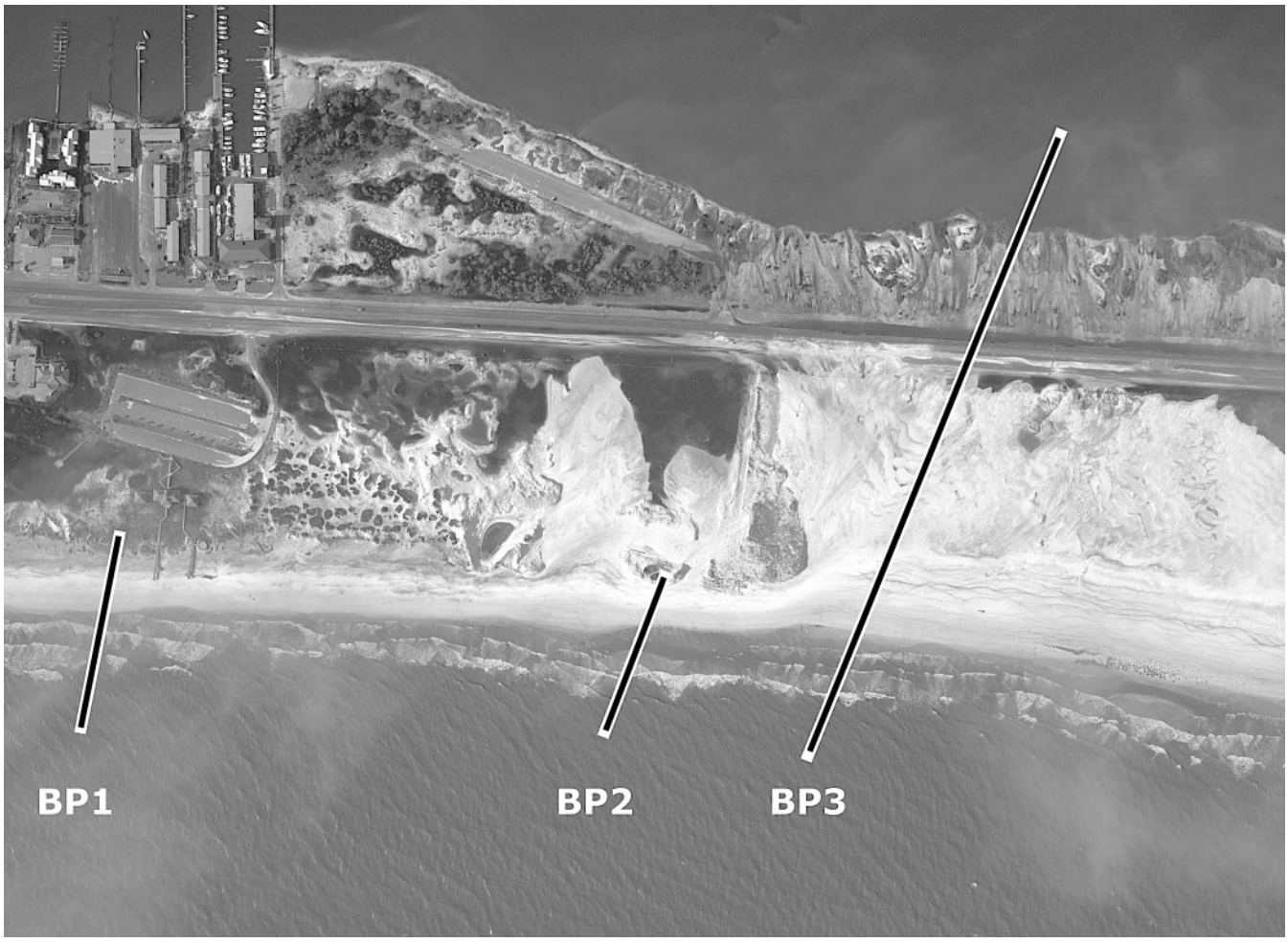

Figure 2. Aerial photo of the westernmost study site, S1_BP, showing the locations of beach profiles BP1, BP2 and BP3. Photo was taken 2 d after the storm, on September 19, 2004. Note the extensive overwash in central and eastern portion of the photo. Photo courtesy NOAA.

landfall, or 110 km from the eastern eyewall. Significant and extensive dune erosion occurred at this site, damaging nearly all the wood overwalks (Figure 3). An array of four trenches was established to examine the subaerial storm deposit.

The third study site is located at Seagrove Beach (S3_SB), roughly 160 km east of the storm center, or 120 km from the eastern eyewall. An array of five trenches was excavated. The Seagrove site is considerably different from the other sites in that the erosion into the Pleistocene dune field exposed layers of dark, heavy minerals, including ilmenite, staurolite, kyanite, zircon, and rutile (STAPOR, 1973; USDA-SCS, 1989). Several layers of the heavy minerals were exposed, with the bottom one located just beneath the present backbeach. Dark, heavy minerals were distributed rather extensively on the surface of the beach (Figure 4). DOUGHERTY, FITZGERALD, and BUYNEVICH (2004) and BUYNEVICH, FITZGERALD, and VAN HETEREN (2004) found that heavy mineral layers tend to concentrate at the base of storm deposits and correlate well with prominent layering in ground penetration radar profiles.

The fourth site is located at Inlet Beach (S4_IB), 175 km east of the storm center, or 135 km from the eastern eyewall. Three profiles were surveyed at this site (Figure 5). The first beach profile (S4_IB1) is bordered landward with a relatively high and vegetated dune. The second profile (S4_IB2) extends seaward from the corner of a high-rise building with no significant dunes in front. The third profile extends across a low-lying area that was overwashed during the storm (Figure 5).

The fifth site is located at Laguna Beach (S5_LB), 180 km east of the storm center, or 140 km from the eastern eyewall. Compared to the west four sites, dune erosion at the Laguna Beach site is much less severe. The dune scarps are typically low and discontinuous (Figure 6). An array of five trenches was excavated to examine the characteristics of the storm deposit.

The sixth site is located on St. Joseph Peninsula (S6_SJ), 240 km east of the storm center, or 200 km from the eastern eyewall. In contrast to the previous east-west-oriented five sites, St. Joseph Peninsula is oriented roughly north-south, and protrudes approximately 60 km farther south into the Gulf of Mexico (Figure 1). STAPOR (1973) found that quartz beach sands in the St. Joseph Spit region contain on average 0.1% heavy minerals by weight. One cross-island profile (S6_SJ1) and one beach/dune profile (S6_SJ2) were surveyed (Figure 7). Significant structural damage to the residential buildings occurred in the vicinity of S6_SJ2, largely because of the narrow and erosional nature of the prestorm beach. No significant overwash occurred on the island, probably due in large part to its well-established dune field in conjunction with the island's long distance from the hurricane center. Two trenches were excavated at S6_SJ1 and three at S6_SJ2.

The seventh and easternmost site is located on St. George Island (S7_SG), 300 km east of the storm center, or 260 km from the eastern eyewall. The island is oriented roughly northeast-southwest, and protrudes approximately 80 km farther south into the Gulf of Mexico, as compared to the western five sites. Two beach profiles were surveyed (Figure 8). The first profile, S7_SG1, extends from the base of a 3-story building with no frontal dune. The second profile, S7_SG2, has a low artificial dune in front.

METEOROLOGICAL AND OCEANOGRAPHIC CHARACTERISTICS OF HURRICANE IVAN

Hurricane Ivan, a large Category 4 hurricane that decreased to a strong Category 3 at landfall, came onshore with tremendous wind, wave and storm surge. Figure 9 shows the wind conditions at landfall as forecasted by the National Hurricane Center, and measured wave and surge conditions at the study sites as the hurricane approached the coastline. Wave data from three National Data Buoy Center (NDBC) offshore wave buoys were examined. A number of tide gages are present in the study area. Three gages are included in Figure 9. These gages are close to the open Gulf, and therefore should provide reliable surge measurements. ?2

At landfall, the sustained hurricane-force wind extended 170 km from the center of the hurricane, as forecasted by the National Hurricane Center. The western four study sites lie within the zone impacted by hurricane- force wind. The sustained tropical storm strength wind extended 475 km from the hurricane center, an area that included all the study sites (Figure 9). It is worth noting that wind conditions changed rapidly as the storm approached the coast. Figure 9 provides a snapshot at landfall.

Significant surge was measured at all the study sites, with a decreasing trend eastward, as expected. In Figure 9, zero hour represents the time of landfall. At the Pensacola tide gage, located approximately 60 km east of S1, the highest surge measured was 2.06 m above the Mean Low Low Water (MLLW). This exceeded the capacity of the gage. Many qualitative pieces of evidence, *e.g.,* deposits of debris flow and a hanging boat anchor as shown in Figure 10, indicate that the storm surge exceeded 2.06 m, even a considerable distance east of Pensacola.

At Panama City Beach, the tide gage is located along the Gulf beach, about 4 km east of S5, or roughly in the center of the study area. The highest surge was measured at 1.96 m above MLLW, nearly four times the typical tidal range. Surge levels above 1.5 m (MLLW) persisted for over 10 hours, and above 1.0 m (MLLW) for 26 hours (Figure 9). The Panama City gage is located within St. Andrew Bay, approximately 27 km east of S5. The highest surge was 1.43 m above the MLLW, with 21 hours above 1.0 m. ?3

The Pensacola tide gage stopped functioning at the time of the hurricane landfall. The peak surge measured at Panama City Beach occurred approximately 5 hours after landfall. The peak surge recorded further east at Panama City occurred roughly 10 hours after the hurricane landfall.

Significantly elevated wave heights were measured at the NDBC wave buoys (Figure 9). An eastward decreasing trend was measured, as expected. Shortly before Ivan landfall, waves of 16 m high were measured at the westernmost gage, 42040, which exceeded the upper limit of the gage. At gage 42039, located directly offshore of most of the study sites and approximately 220 km west of gage 42040, the highest measured wave was 12 m. For 17 hours, wave heights exceeded 10 m (Figure 9), which is over 10 times the average wave height in this region. Gage 42036 is approximately 150 km east of gage 42039 and roughly due south of S7_SG. The highest measured wave was 6.4 m, and wave heights exceeding 5

Figure 3. Study site S2_GVH. Upper: dune scarp with white line indicates prestorm dune level at the walkover structure (distinguished by the different color of the wood); lower: extensive dune scarp and locations of the trenches. Photo was taken on October 17, 2004, 30 d poststorm.

Figure 4. Study site 3_SB. Note the high concentration of dark heavy minerals on the beach, which is considerably different from the white sand at the rest of the study sites. Photo was taken on October 17, 2004, 30 d poststorm.

m persisted for 29 hours (Figure 9). The highest waves at all three buoys were measured shortly before landfall. These extremely energetic offshore wave conditions lasted through the landfall.

In addition to storm surge as measured by the tide gages, further elevated water levels along the beach can be caused by wave setup and swash run-up. Various methods, as discussed in the following section, are available to calculate the wave setup and swash run-up. In the following discussion, the elevated water level is estimated based on the measured surge height in addition to the calculated wave setup and swash run-up. This elevated water level is compared with the measured vertical limits of morphological changes.

METHODOLOGY

Morphological impact of Hurricane Ivan is quantified through a time-series survey of the beach/dune and cross-island profiles. Standard level-and-transit survey procedures were followed using an electronic total station (WANG and DAVIS, 1998). The prestorm survey was conducted 1.5 days before the landfall, on September 14, 2004. The large study area was selected based on the path of the hurricane as projected 2 days before landfall. The first poststorm survey was conducted roughly 1 week after the impact. The second and third poststorm surveys were conducted roughly 4 and 11 weeks after storm impact, respectively. Because of the rough sea conditions before the impact, the beach-profile survey was terminated at approximately 1 m water depth. Therefore, the present analysis pertains mostly to the beach/dune changes. All the beach-profile surveys are referenced to the National Geodetic Vertical Datum (NGVD), which lies approximately 0.2 m below the present sea level. Continued beach-profile surveys are being conducted. However, long-term beach/dune recovery is beyond the scope of this paper. ?4

Beach characteristic and dune scarp measurements were conducted at most of the study sites. The width of the beach

Figure 5. Study site S4_IB. Upper: the western portion of the site and beach profiles IB3 and IB2. Lower: the eastern portion of the study site and the profiles IB2 and IB1. Photo was taken 11 wk after the Ivan impact.

Figure 6. Study site S5_LB. The beach scarp in the middle of the photo is not related to the storm. The dune scarp was caused by the storm impact. Photo was taken a month after the impact.

Figure 7. Study site S6_SJ2 at St. Joseph Peninsula looking north. The white line shows the prestorm dune level at the dune walkover (indicated by the different color of the wood). Photo was taken on September 23, 2004, a week after the Ivan impact.

Figure 8. Study site S7_SG. Profile S7_SG1 is located toward the top of the photo and S7_SG2 at the bottom. Minor dune scarping occurred at this site. Photo was taken on September 23, 2004, 1 week after Ivan impact.

was measured from the inferred high tide line to the base of the first dune. The prestorm beach width was determined from the surveyed profiles at S1_BP, S4_IB, S6_SJ, and S7_SG. Poststorm beach width measurements were conducted, using a measuring tape, at all the study sites except S2_GVH. The goal of these measurements was to examine qualitatively the relationship, if any, between the beach width and the degree of dune erosion. Location of the high tide line was inferred in the field by the presence of a fresh debris line roughly parallel to the waterline. The orientation of this line was then measured using a Brunton compass.

Dune-scarp heights were also measured, and descriptions of scarp characteristics such as continuity and orientation were recorded. The measurement points were selected based on four criteria: (1) close proximity to the water line; (2) presence of sedimentary structures; (3) continuity of the scarp; and (4) proximity to the trenches (discussed in the next paragraph). Height of the dune scarp was measured at the troughs and at the crest of a scarp anticline, and then averaged. Strike of the scarp was measured with a compass, along with an estimation of the scarp continuity. Qualitative features were noted at each measurement site, including sand color and composition, shell and organic material compositions, degree of bioturbation, characteristics of sediment structures, and minor washover features.

In order to apply the SALLENGER (2000) scale, it is crucial that the R_{HIGH} value be estimated accurately. The representative high elevation of the landward margin of swash, R_{HIGH}, is composed of three components: storm surge, wave setup, and swash run-up. Typically, storm surge can be measured at the numerous tide gages and is reasonably well monitored by the US National Ocean Services. However, wave setup and swash run-up along the beach cannot be measured by the existing tide gages. Several studies were conducted to study the limit of wave setup and swash run-up. GUZA and THORNTON (1980, 1981, 1982) found that along dissipative beaches the wave setup (R) is linearly proportional (17%) to the offshore significant wave height (H_o) and the swash run-up is dominated by low-frequency oscillations:

$$R = 0.17H_o. \tag{1}$$

SALLENGER and HOLMAN (1985) and HOLMAN (1986) developed an empirical model as:

$$R_{2\%} = H_o(0.83 \times \zeta_o + 0.2) \tag{2}$$

where $R_{2\%}$ is the 2% exceedence run-up including both wave setup and swash run-up. H_o is deep-water significant wave height, and the Iribarren number (or surf similarity parameter)

$$\xi_0 = \frac{\beta}{\sqrt{\frac{H_o}{L_o}}} \tag{3}$$

where β is local beach slope and L_o is deep-water wavelength. SALLENGER (2000) suggested that

$$R_{HIGH} = R_{2\%} + \eta_{mean} \tag{4}$$

$$R_{LOW} = R_{HIGH} - S_{2\%} \tag{5}$$

where η_{mean} is the height of storm surge, and $S_{2\%}$ is the 2% exceedence swash amplitude that can be calculated, based on HOLMAN (1986), as

$$S_{2\%} = H_o(0.85\chi_o + 0.06). \tag{6}$$

RUGGIERO *et al.* (2001), based on a similar dataset to that of HOLMAN (1986) and some additional data from the Oregon coast, developed an empirical relationship as

$$R_{2\%} = 0.27(\beta H_o L_o). \tag{7}$$

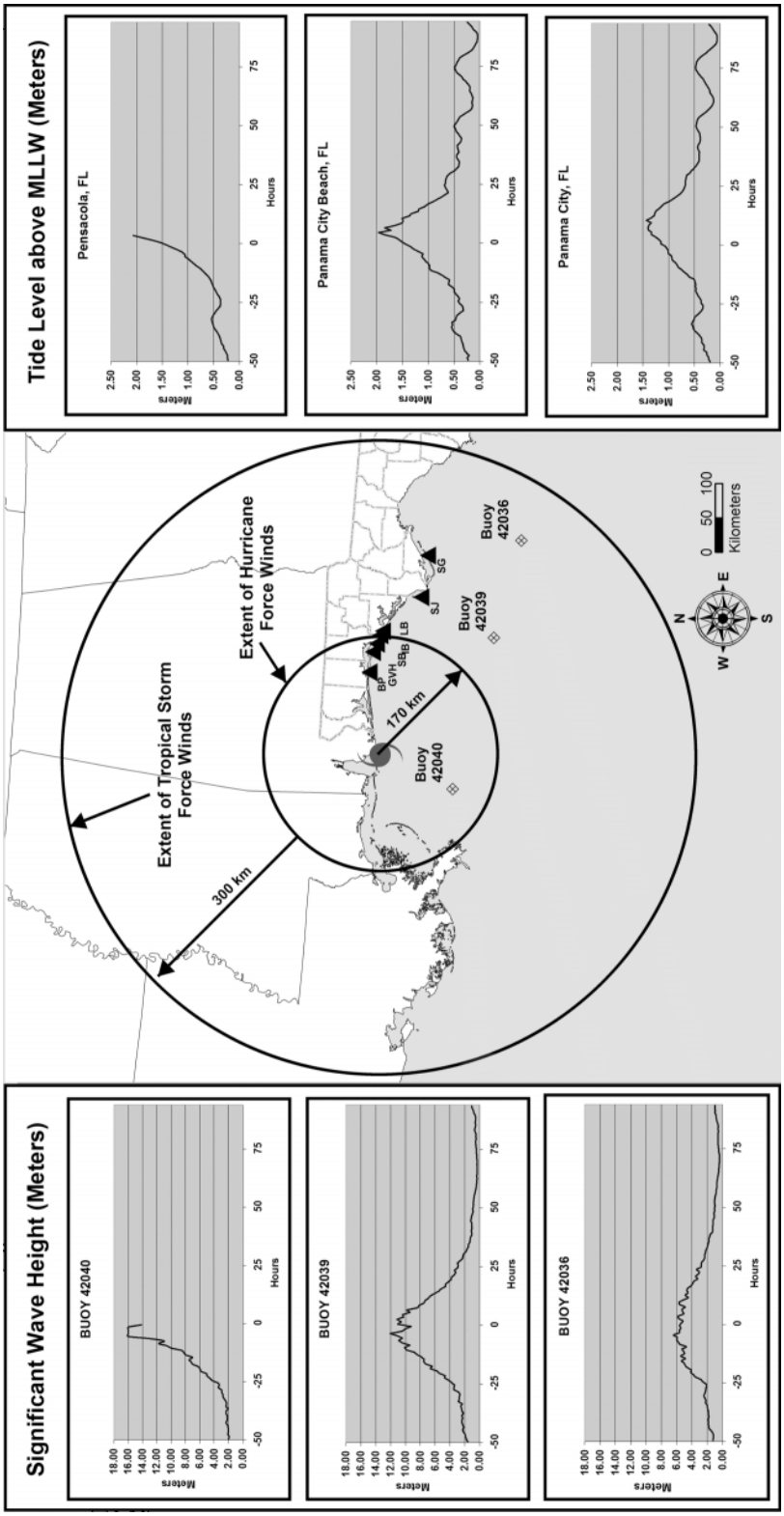

Figure 9. Forecasted extent of sustained hurricane-force and tropical-storm-force winds just before landfall, and measured offshore wave heights and coastal storm surges.

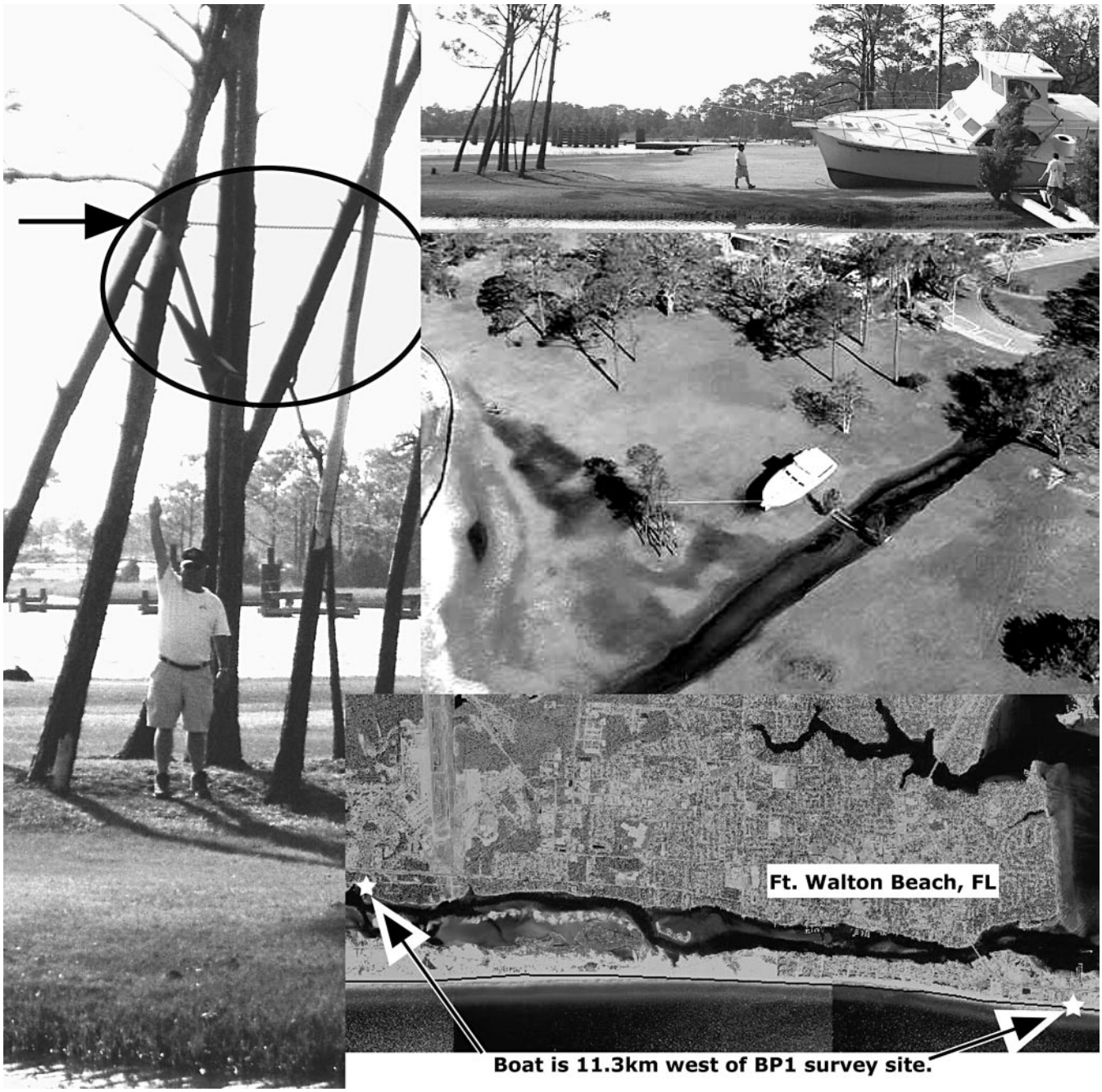

Figure 10. A grounded large yacht indicating that this area was under considerable depth of water. The anchor chain (black arrow) is wrapped around a tree at approximately 4 m above ground level. The ground at this location is approximately 1 m above the water level of the Santa Rosa Sound.

The above equations, which were largely developed based on studies along the US Pacific and Atlantic coasts, are used to calculate the wave setup and swash run-up. Their applicability along the Gulf coast is discussed based on comparisons with the measured elevations of significant beach erosion.

Characteristics and thickness of the subaerial storm deposits on the backbeach were studied in 46 trenches excavated in all the seven sites. Twelve shore-perpendicular transects of trenches were examined along the entire study area. Nine of the transects were located along the surveyed beach profiles. Most of the trenches were spaced approximately 5 m apart extending from near the toe of the dune (or dune scarp) toward the Gulf of Mexico. Trenches located on overwash fans were spaced much further apart depending on cross-shore extent of the washover. At each trench, Ivan-induced deposits were identified, described, photographed, and

measured. In the middle part of the two studied washover fans, the trenches did not reach the bottom of the storm deposits. The objectives of the trench study were to (1) quantify the thickness of the subaerial storm deposits; (2) examine the trends of the storm deposits, both cross-shore and along the studied coast; and (3) characterize the sedimentary structures and textural properties of the pre- and poststorm deposits. This part of the study emphasizes the depositional aspect of the storm over the subaerial beach, which is often overshadowed by the more obvious and dramatic erosional aspect.

RESULTS AND DISCUSSION

Beach/Dune Erosion

Significant beach/dune erosion was measured at all the study sites, extending from Ft. Walton Beach to St. George Island over 300 km east of the storm center at landfall (Figure 11). The elevation of the landward limit of beach/dune erosion demonstrated a decreasing trend eastward, as expected. At the westernmost site, S1_BP1, the frontal dune of nearly 5 m above NGVD was eroded by Ivan (Figure 11). NGVD 0 is roughly equal to mean low tide in the study area. The pre-Ivan survey was conducted 10 days before the poststorm survey. There is little doubt that the erosion was directly caused by Ivan. The high dune at S1_BP2 is located at the edge of a dune field (Figure 2). Substantial dune erosion in the form of dune face retreat occurred. The dune survived the hurricane impact, although its surrounding area was overwashed (Figure 2). The different responses at S1_BP1 and S1_BP2 indicate that the continuity of the dune field plays a significant role during hurricane impact.

At S4_IB, the elevation of the landward limit of beach erosion reached approximately 4 m above NGVD (Figure 11). A slightly higher landward limit was measured at S4_IB1, where a frontal dune system exists, as compared to S4_IB2, directly in front of a high-rise building (Figure 5). However, the elevation (3.5 m) of the bottom of the dune scarp at S4_IB1 roughly equals the highest elevation (3.3 m) of the prestorm backbeach at S4_IB2. Therefore, the highest elevation of Ivan-induced beach/dune erosion reached approximately 3.5 m NGVD at Site 4.

At S6_SJ, no overwash occurred at the cross-island profile, apparently because of the protection of the high dune and reduced hurricane forcing farther away from the center (Figure 11). Significant erosion occurred on the backbeach at S6_SJ1. Ivan eroded over 40 m of backbeach with a relatively uniform elevation of approximately 1.5 m, whereas minimal damage occurred at the frontal dune system. Profile S6_SJ2, approximately 3 km north of S6_SJ1, reacted very differently, with the development of a 1.5-m-high dune scarp. Substantial structural damage to the frontal residential buildings occurred in the S6_SJ2 area. The more apparent erosion at this location is related to the fact that the beach was quite narrow before the storm impact. The elevation of the bottom of the erosional scarp is roughly 1.6 m, similar to the vertical erosional limit at S6_SJ1. Therefore, the Ivan erosion reached approximately 1.6 m at Site 6, considerably lower than the western sites, as expected.

Substantial erosion was measured at the easternmost study site, S7_SG, which is over 300 km away from the storm center at landfall. Overall, an elevation loss between 0.3 and 0.7 m was measured over the 40-m-wide stretch of backbeach. The highest elevation near the landward limit of the beach erosion is 2.0 m at S7_SG1 and 2.8 m at S7_SG2. A small dune scarp developed at S7_SG2. The elevation at the bottom of the scarp is 2.3 m, similar to the erosional elevation at S7_SG1. Therefore, the Ivan erosion reached approximately 2.3 m above NGVD.

Extensive dune scarping occurred in the study area. The scarp height and lateral extension, poststorm beach width, and vertical erosional limit as discussed earlier are summarized in Table 1. The overall trend across the study area shows that the height and lateral extent of dune scarping generally decrease away from the storm center, as expected. However, the dune scarping is influenced by many morphological factors in addition to the intensity of the storm impact. Some of the factors include: the geometric characteristics of the dunes, the lateral extension and the vegetation coverage, the elevation of the dune toe, and the width and elevation of the beach in front of the dune. For example, the high dune scarp at S6_SJ2, as compared to the neighboring S6_SJ1, is likely related to the narrow frontal beach. The very high dune scarp at S1_BP2 is probably related to the isolation of that dune.

Volume changes over the dry beach (above NGVD 0) and dune field were calculated and listed in Table 1. Substantial erosion, *i.e.,* volume loss, occurred at all the study sites, as expected. The greatest volume change, nearly 100 m^3/m loss, was measured at S1_BP2. The adjacent S1_BP1 lost 56 m^3/m. The substantial dune-face erosion at S1_BP2 contributed to the large volume loss (Figure 11). At S4_IB, volume loss of 35 and 47 m^3/m occurred at the two profiles, respectively. At S6_SJ, 40 m^3/m loss was measured at S6_SJ1 and 32 m^3/m at S6_SJ2. Much less beach erosion, 15 and 19 m^3/m loss, occurred along the two profiles at S7_SG.

It is worth noting that S6_SJ is oriented north-south, in contrast to the general east-west orientation of the northern Gulf coast. The beach is roughly parallel to the storm track, and therefore parallel to the wind direction (from south to north). This study site was selected to examine the influence of beach orientation on storm impact. Although the two study locations are not adequate to draw solid conclusions, the lower erosional limit of 1.6 m, as compared to the 2.3 m at S7_SG further east, is probably related to the regional beach orientation. No significant difference in beach-profile shape can be identified, possibly because of the limited amount of data. The initial hypothesis was that significant longshore transport should occur because of the parallel orientation of the island to the storm track. However, no solid evidence of longshore sand redistribution, *e.g.,* substantial growth of spit or northward migration of the northern end of the barrier island, is apparent on aerial photography. The relatively large beach-volume loss (Table 1) may be related to longshore transport.

Overwash

Extensive overwash occurred at the westernmost site, S1_BP, and caused substantial damage to the four-lane US

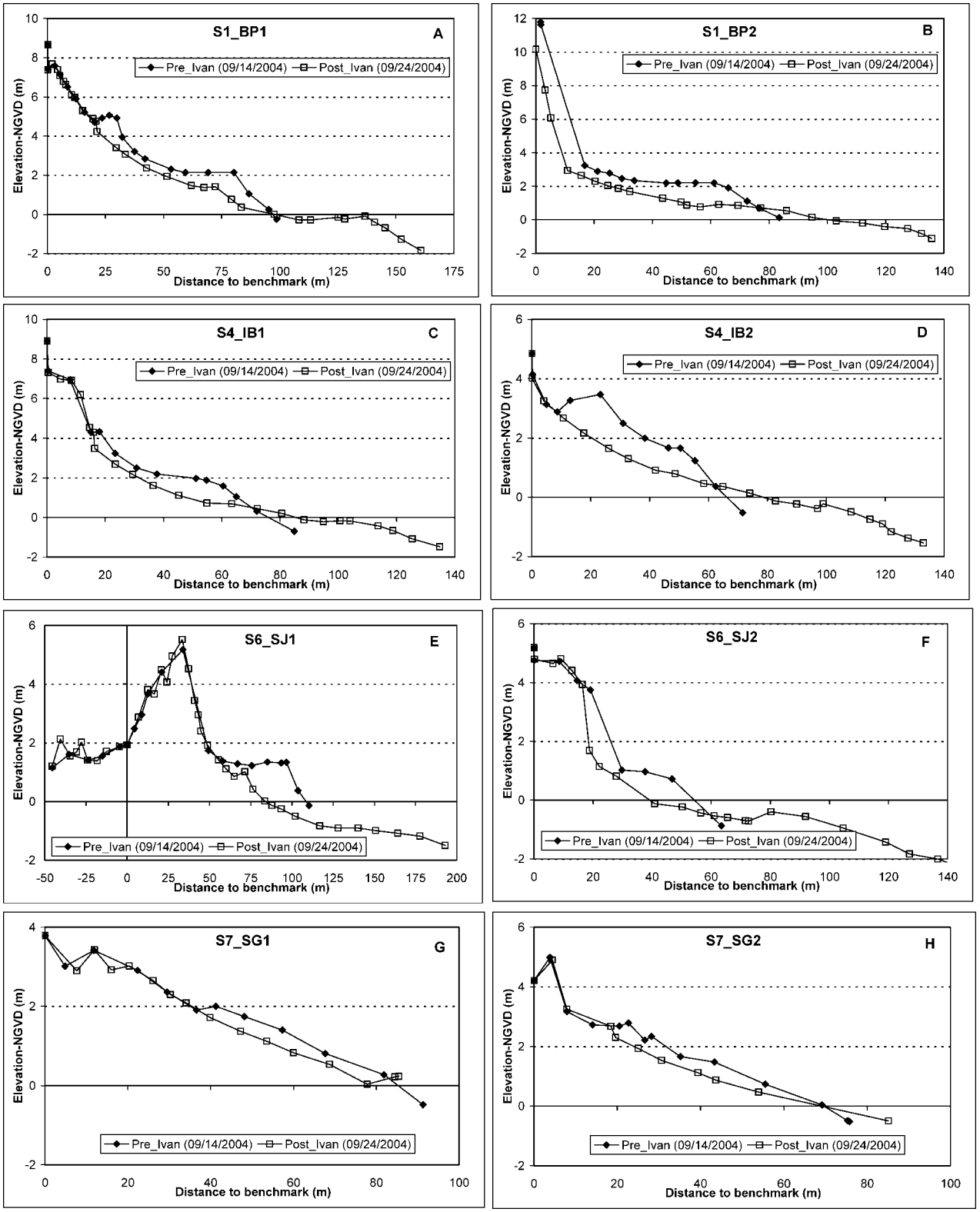

Figure 11. Pre- and poststorm beach/dune profiles at the study sites. Significant erosion was measured at every location.

Table 1. *Height and characteristics of dune scarps and pre- and portstorm beach volume change (negative indicates volume loss). The volume change is calculated between NGVD 0 and the highest elevation of erosion, and therefore represents the changes on the dry beach and dune field.*

Location	Scarp Height (m)	Beach Width (m)	Erosional Limit (m)	Distance to Eastern Eyewall (km)	Local Beach Orientation (°)	Alongshore Extension of Dune Scarp	Pre- and Poststorm Beach Volume Change (m^3/m)
S1_BP1	5.2	45.0	5.0	80	98	continuous	−56
S1_BP2	7.3	41.5	5.0	80	98	end of dune field	−97
S2_GVH	no data	27.5	no data	110	110	continuous	no data
S3_SB	4.3	31.0	no data	120	124	continuous	no data
S4_IB1	0.9	34.7	3.5	135	118	continuous	−35
S4_IB2	no data	no data	no data	no data	no data	no dune	−47
S_5LB	0.7	49.0	no data	140	126	discontinuous	no data
S_6SJ1	0.7	45.0	1.6	200	164	discontinuous	−40
S_6SJ2	3.5	25.5	1.6	200	161	continuous	−32
S7_SG1	1.1	22.9	2.3	260	68	discontinuous	−15
S7_SG2	no data	no data	no data	no data	no data	discontinuous	−19

Highway 98. Further west extending to the western tip of Santa Rosa Island and the Gulf Shores in Alabama, extensive overwash and inundation dominated the storm impact (Figure 12). The intensity of overwash decreased rapidly east of S1_BP. Scattered overwash occurred at some of the low-lying eastern study sites, *e.g.,* at S4_IB3. Overwash occurred at two of the three cross-island profiles (Figure 13). Overwashed area typically exhibited significant beach erosion along the Gulf side, and substantial accumulation and flattening along the bay side.

Severe beach and dune erosion occurred at S1_BP3 (Figure 13). The prestorm frontal dune of up to 3.6 m above NGVD was completely eroded, along with the erosion of the entire Gulfside backbeach. The elevation of the prestorm backbeach was higher than 2 m. An elevation loss of 1 to 2 m occurred Gulfward from the prestorm frontal dune. The erosion of the 3.6-m-high dune agrees with the 5-m vertical erosional limit as detected from the adjacent beach-profile changes (Figure 11). Comparing the pre- and post-Ivan profiles, it is apparent that the sand eroded from the Gulf beach and frontal dune was deposited in the relatively low-lying region immediately landward of the frontal dune. The overwash platform is over 200 m wide with an elevation of approximately 2.6 m. Across the entire 550-m profile, approximately 20 m^3/m of sand were lost when comparing the pre- and poststorm profiles. This resulted from 126 m^3/m loss along the Gulfside beach and 106 m^3/m gain on the overwash platform. This indicates that the sand eroded from the Gulfside beach was largely overwashed and deposited immediately landward, with minimal net sand loss to the offshore region. A similar pattern of erosion and

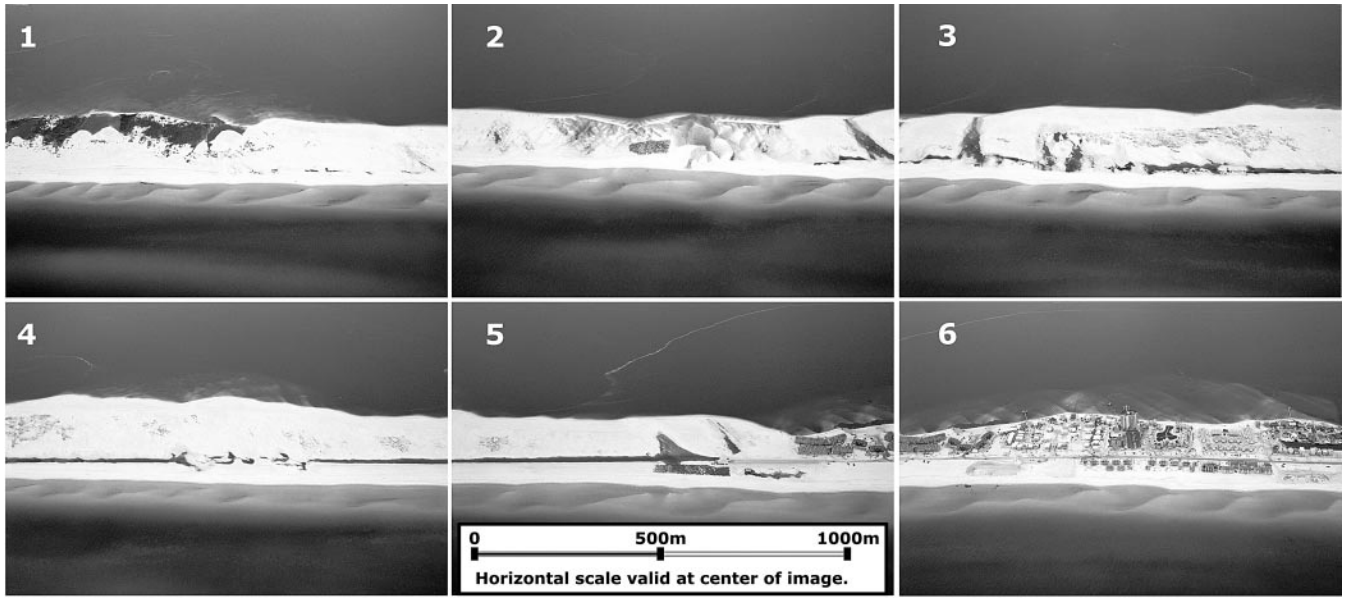

Figure 12. Extensive overwash and inundation at the western end of Santa Rosa Island. Each oblique image is approximately 1200 m wide at the center of the frame. The images are sequenced from west to east. Frame number 5 overviews the entrance to the Santa Rosa State Park. Nearly the entire park was inundated. Photo date is December 4, 2004, nearly four months after the impact.

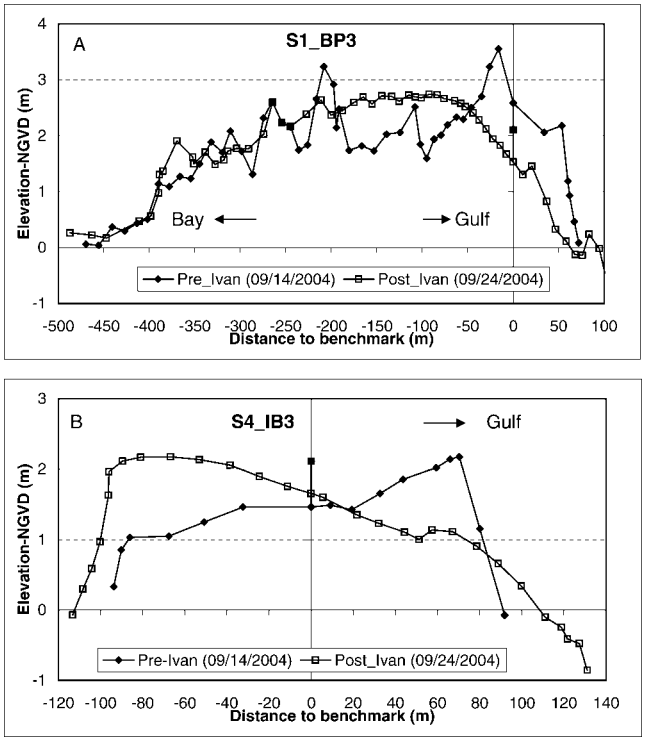

Figure 13. Overwash at S1_BP3 and S4_IB3. Note the significant erosion along the Gulfside backbeach.

deposition of barrier-island overwash was also reported by STONE and WANG (1999), STONE *et al.,* (1999, 2004), and SALLENGER (2000).

The morphological change at S4_IB3 was considerably different from that at S1_BP3 (Figure 13), probably because of the different prestorm profile characteristics and the relative storm intensity. The elevation of the washover platform increased landward, reversing the prestorm landward-dipping profile to the poststorm seaward-dipping profile. Across the 200-m stretch of the beach, a net gain of 50 m^3/m sand was measured after the storm impact. This resulted from 34 m^3/m loss along the Gulf side beach and 84 m^3/m gain on the overwash platform. Longshore sand transport may be responsible for this net volume gain. The small inlet migrated considerably to the west and was closer to the relict pier (Figure 5, upper) after the storm. It is worth noting that S4-IB3 is located near a small inlet that has been artificially maintained for water quality purpose for the small back bay and does not represent the typical beach response in this area.

Beach/Dune Erosion and Elevated Water Level

Study site S4_IB is located approximately 10 km west of the tide gage (facing the Gulf) at Panama City Beach (Figure 9). The highest surge measured at this tide gage was slightly less than 2.0 m above the MLLW. Substantial beach/dune erosion was measured at 3.5 m above NGVD (NGVD is roughly 0.1 m above MLLW in this area), or about 1.6 m above the highest surge measured. S1_BP is located approximately 60 km west of the Panama City Beach tide gage and 60 km east of the Pensacola gage. The limit of the Pensacola gage was exceeded when the surge reached 2.1 m. Given that the 2.1 m surge was reached almost at the time of landfall (Figure 9), it is reasonable to assume that the surge did not substantially exceed the 2.1 m limit. Also, the Pensacola gage is located inside Pensacola Bay and not directly facing the Gulf. Substantial erosion was measured at nearly 5 m above NGVD, or nearly 3 m above the highest surge measured. It is not likely that the storm surge alone reached to the elevation of the erosional limit at both S1_BP and S4_IB. Wave setup and swash run-up must have played a significant role in further elevating the water level.

As discussed in the previous sections, several empirical methods (Equations 1 through 7) have been established to estimate the level of wave setup and swash run-up. Here, these equations are used to calculate the wave setup and swash run-up and the results are compared with the water level deduced from the morphological changes. It is reasonable to assume that the water reached at least to the level of significant morphological changes, *i.e.,* the vertical erosional limit as discussed in the previous sections.

Wave buoy 42039 is approximately offshore of sites S1_BP through S5_LB. The average wave height between 8 hours before and 4 hours after landfall is used in the calculation. The averaging is slightly skewed to before the landfall in order to account for the time the waves needed to travel onshore from the considerable offshore distance (Figure 9). The average significant wave height is 10.6 m and average peak period is 13.4 seconds. Based on linear wave theory, the deepwater wavelength can be calculated as

$$L_o = \frac{gT^2}{2\pi} \tag{8}$$

where g is the gravitational acceleration. Corresponding to the 13.4-second wave period, the deepwater wavelength is 280 m. The beach slope and Iribarren number (Equation 3) are calculated based on prestorm survey data. The slope of the foreshore, extending from the berm crest to the low-tide line, is used. It is worth noting that both beach slope and Iribarren number are significantly different before and after the storm. Also, the wave buoys are well over 100 km offshore and may not directly represent the deep-water wave conditions of the study sites. At the easternmost site, S7_SG, wave data from buoy 42036 (average H_o = 5.7 m; T_p = 12.0) were used. The purpose of the present exercise is to provide an order-of-magnitude estimate of the overall water level and to compare the calculated value with the level of significant erosion. No data from the Gulf of Mexico coast were available during the development of the empirical wave setup and swash run-up formulas (Eqs. 1 through 7). It is important to test their general applicability along the storm-prone northern Gulf coast.

The calculated wave setup and swash run-up using the various equations are summarized in Table 2. Equations 2, 6, and 7 yielded wave setup and swash run-up of nearly 5 m to over 8 m. Compared to the values estimated from the morphological changes, also listed in Table 2, the calculated values are 3 to 6 m greater. The steep foreshore slope, and there-

Table 2. *Calculated wave setup and swash runup. The measured values are obtained by subtracting the measured surge level from the highest elevation of erosion.*

Location	H_o (m)	T_p (s)	L_o (m)	Foreshore Slope	Surf Similarity	Measured Values (m)	Eq. 1 (m)	Eq. 2 (m)	Eq. 6 (m)	Eq. 7 (m)
S1_BP1	10.6	13.4	280	0.14	0.72	<2.8*	1.8	8.5	7.1	5.5
S1_BP2	10.6	13.4	280	0.10	0.51	<2.8*	1.8	6.6	5.3	4.7
S4_IB1	10.6	13.4	280	0.10	0.51	1.5	1.8	6.6	5.3	4.7
S4_IB2	10.6	13.4	280	0.10	0.51	1.5	1.8	6.6	5.3	4.7
S7_SG1	5.7	12.0	225	0.05	0.31	0.7	1.0	2.6	1.9	2.2
S7_SG2	5.7	12.0	225	0.06	0.38	0.7	1.0	2.9	2.2	2.4

* The Pensacola tide gage reached its 2-m limit at Ivan landfall (Figure 9). The 2-m surge is used here. However, it is reasonable to believe that the surge exceeded 2 m; therefore, the wave setup and swash runup should be less than 2.8 m.

fore the relatively large Iribarren number, contributed significantly to the large calculated values. The above formulas were developed mostly based on data from dissipative beach with gentle beach slope and small Iribarren number. Although the studied coast has gentle offshore slope, the foreshore tends to be relatively steep, controlled by the dominant locally generated short-period waves. The much lower predicted numbers at S7_SG1 and S7_SG2 are directly related to the gentler foreshore slope. The gentler slope at the St. George Island sites is likely resulted from the earlier impact of Hurricane Frances. Frances, a tropical storm at landfall, came onshore approximately 80 km west of the St. George Island study sites.

Equation 1 yielded much smaller numbers of 1–2 m because the beach-slope term is not included. Results from this simple equation also compare well with the measured morphological changes. Predictions from the other equations exceeded the elevation of morphological changes by a large margin. Practically, given the usually complicated nearshore bathymetry (*e.g.,* presence of nearshore bars), beach slope is a difficult parameter to accurately define and determine. In addition, beach slope responds rapidly with wave-energy and water-level variations. This is well demonstrated by the significant slope changes before and after the storm impact, as well as the rapid slope "recovery" after the storm as discussed in the section after next.

Thickness and Trend of Subaerial Storm Deposition

As demonstrated by the pre- and poststorm beach profiles, the overall net impact of the storm to the barrier beaches was apparently erosional. Elevation losses on the backbeach ranged from approximately 0.4 m at S7_SG to over 1.5 m at S1_BP. However, observations made in the 46 trenches on the poststorm backbeach and overwash platform revealed that considerable sedimentation also occurred during or immediately following the storm event.

In most of the trenches, a sharp, mostly planar erosional surface separates the prestorm sediment from the storm layer (Figure 14). However, in certain cases distinguishing the prestorm sediments from the storm deposits remained problematic. This was most evident in trenches located proximal to the high tide line, where little to no textural or color variations exist between pre- and poststorm deposits. Also, the present trench study was conducted 30 days following the storm impact, and considerable poststorm beach recovery had occurred seaward of the high tide line (as discussed in the next section). Trenches on the overwash platforms in places could not be excavated deep enough to expose prestorm deposits because of locally thick overwash deposits. Additionally, in areas where the prestorm surface was nonvegetated clean dune sand, the erosional surface was not apparent. Therefore, the present study of storm-layer thickness focuses on the storm deposition in the foredune and backbeach areas situated well above regular high tide (*i.e.,* with little short-term recovery). Numerous studies have been conducted on storm-induced overwash deposits (*e.g.,* LEATHERMAN, WILLIAMS, and FISHER, 1977; LEATHERMAN and ZAREMBA, 1987; MORTON, 2002; MORTON and SALLENGER, 2003; SCHWARTZ, 1975, 1982; SEDGWICK and DAVIS, 2003).

The subaerial storm deposits are characteristic of nearly horizontal planar bedding with little to no bioturbation (Figure 14). Heavy mineral layers and laminae are common, especially at S3_SB, where the supplies from the dunes are abundant (STAPOR, 1973; USDA-SCS, 1984). Buried fresh organic material (Figure 14, S7, upper end of the arrow) locally provides a clear indication of new sedimentation. Erosional truncation can be identified in some cases, especially close to the ocean (Figure 14, S1). Prestorm deposits, especially when near the dune, are typically of a different color, with modestly decayed organic material imparting brownish stains (Figure 14, S2, S4, S5, S7). Sedimentary structures in the prestorm dune deposits are poorly preserved, largely because of intensive bioturbation.

It is reasonable to assume that the storm impact is composed of two phases. The first phase is dominated by erosional regime in response to the sharp increase of wave energy combined with the rising water level associated with the approaching storm. The second phase is dominated by depositional regime, corresponding to the dissipating wave energy and falling water level associated with the waning stages of the storm. In contrast to the well-studied erosional effects of storms, the depositional phase has not been well documented except at places where net deposition occurred during a storm (*e.g.,* COLEMAN, 1978; KEEN and STONE, 2000). As illustrated in Figure 14, although the net result is erosional, substantial subaerial storm deposits occurred, extending over 300 km from the storm center.

The thickness of the subaerial storm deposits was measured in all the trenches in which the erosional boundary could be clearly identified. Generally, the thickness of the

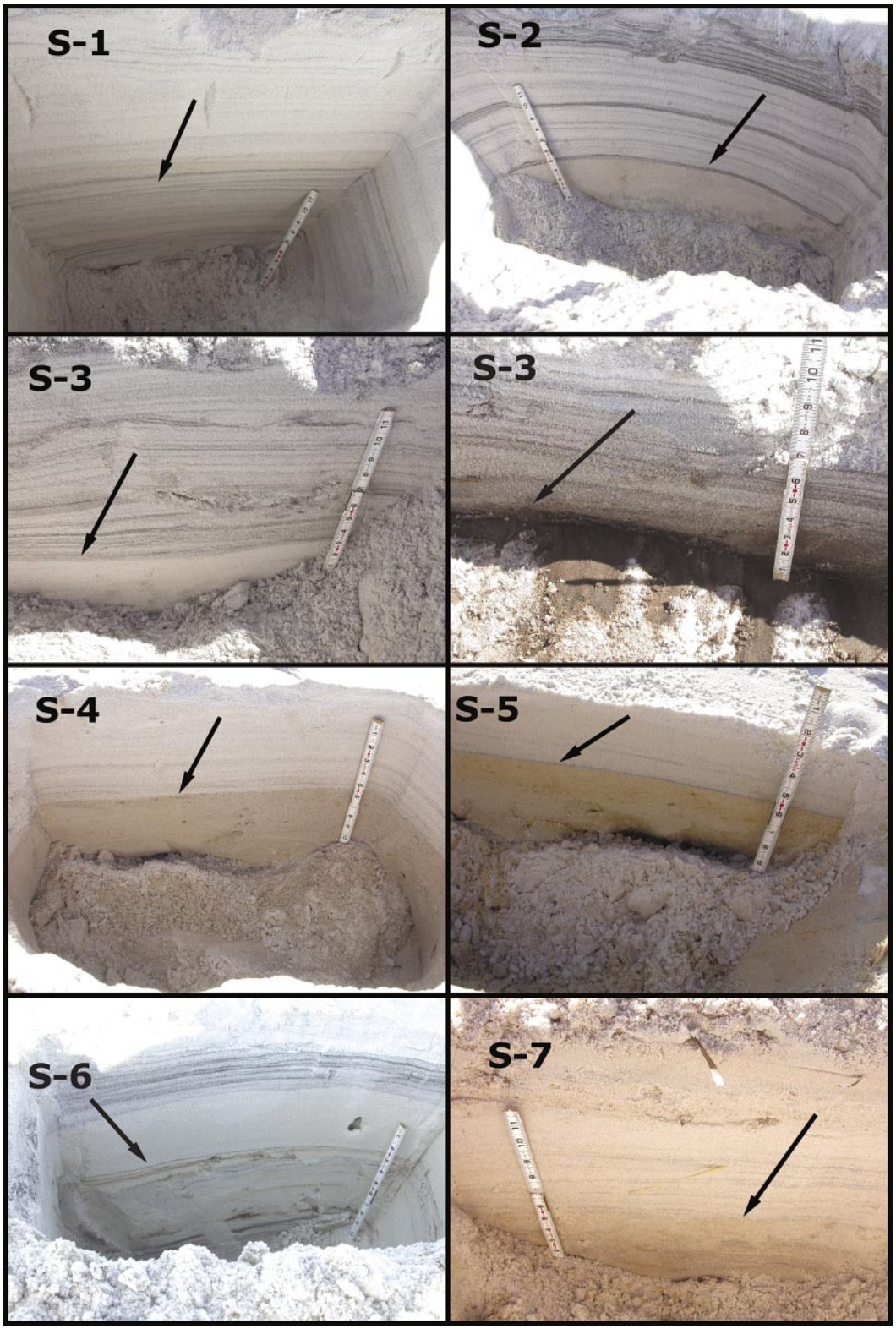

Figure 14. Contacts between post- and prestorm deposits including examples from all the study sites from west to east (S1_BP through (S7_SG). Two examples are given at S3_SB, with the right-side image showing the dark heavy mineral layer at the bottom of the trench.

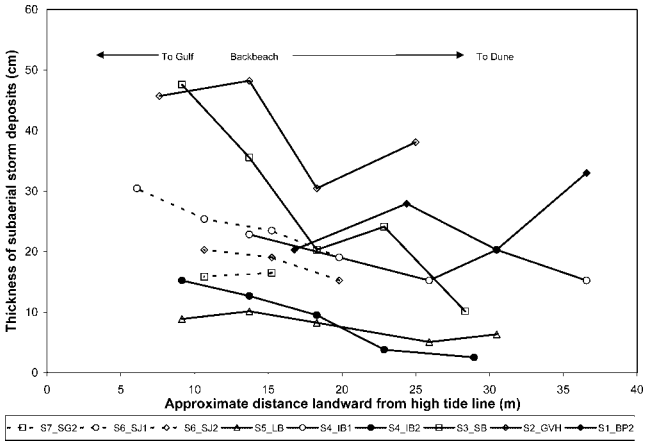

Figure 15. Thickness of storm deposits at all the study sites.

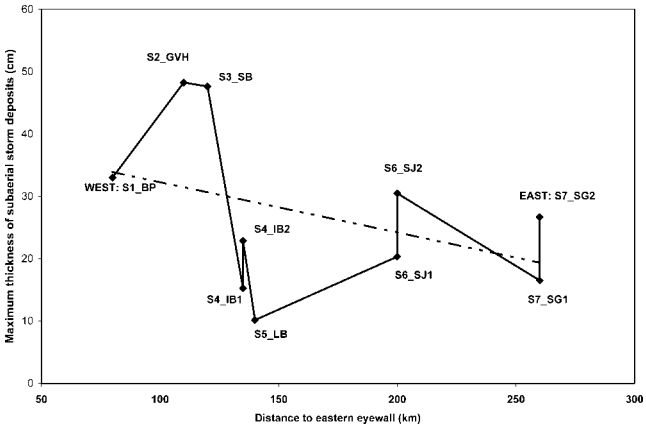

Figure 16. An eastward decreasing trend of the maximum thickness of the subaerial storm deposits.

storm deposit ranged from 10 cm to nearly 50 cm (Figure 15). A general landward thinning trend was measured along most of the trench transects. The landward-most trenches were located approximately 5 m seaward of the poststorm dune field or scarp, except at S7_SG1 and S6_SJ1 where dune scarping was low and discontinuous. At the western sites, S1_BP, S2_GVH, and S3_SB, the landwardmost trench is located within the prestorm dune field. A thicker layer of storm deposit was measured at the landwardmost trenches at S1_BP and S2_GVH. The thicker storm deposit may be attributed to the abundant sand supply from the eroding dune. This trend was not observed at Site 3. The sharp decrease of the storm layer thickness landward was probably caused by the condensed heavy mineral layer (pre-Holocene) at the bottom, limiting the depth of erosion (Figure 14, S3 at the right column).

Figure 16 illustrates the measured maximum thickness of storm deposit at each site versus the distance to the eastern eyewall. An eastward decreasing trend, although with considerable variations, was observed. Slightly thicker storm deposits were measured at the easternmost sites, S6_SJ and S7_SG, as compared to S4_IB and S5_LB. This is probably related to the fact that S6_SJ and S7_SG protrude into the Gulf approximately 60 to 80 km farther than the 5 western study sites (Figure 9). Therefore, the duration of storm impact on S6_SJ and S7_SG may have been prolonged.

Morphological factors, in addition to the storm intensity, may also influence the thickness of the subaerial storm deposits. The maximum storm-deposit thickness was compared to a variety of factors, including post- and prestorm beach slope, dune-scarp height, post- and prestorm beach width, and prestorm berm height. A qualitative relationship can be observed between storm deposit thickness and the poststorm beach width (Figure 17). Thicker storm deposit was measured at narrower beaches, and thinner storm deposit was measured at wider beaches. No convincing relationship can be found between the maximum storm deposit thickness and the other factors examined. The presence or absence of dune scarping does not appear to have any consistent relationship to the storm layer thickness.

Short-Term Poststorm Beach/Dune Recovery

Three poststorm surveys were conducted. The first poststorm survey was conducted on September 24, 2004, 8 days after the landfall on September 16th. The second survey was conducted on October 16, 30 days after the landfall, and the third survey was conducted on December 3, 78 days after the landfall. The purpose of this portion of the study was to examine the short-term beach/dune recovery by natural processes. Continued poststorm study is currently underway, but long-term recovery is beyond the scope of this paper.

Considerable beach recovery, in the form of berm growth, occurred within 90 days after the storm impact at all the study sites (Figure 18). Little to no dune recovery was measured in the short term, as expected. The most apparent beach recovery is the growth of the berm. For all the cases except S7_SG1, the berm crest recovered to prestorm height. For S1_BP and S4_IB, the berm crest recovered to the pre-

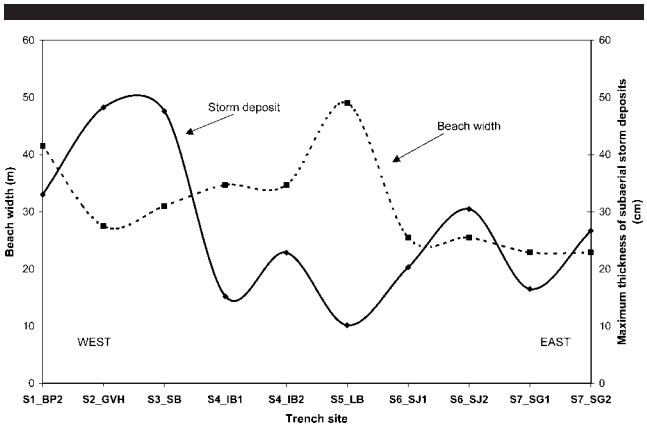

Figure 17. Relationship between beach width and the maximum thickness of the subaerial storm deposits.

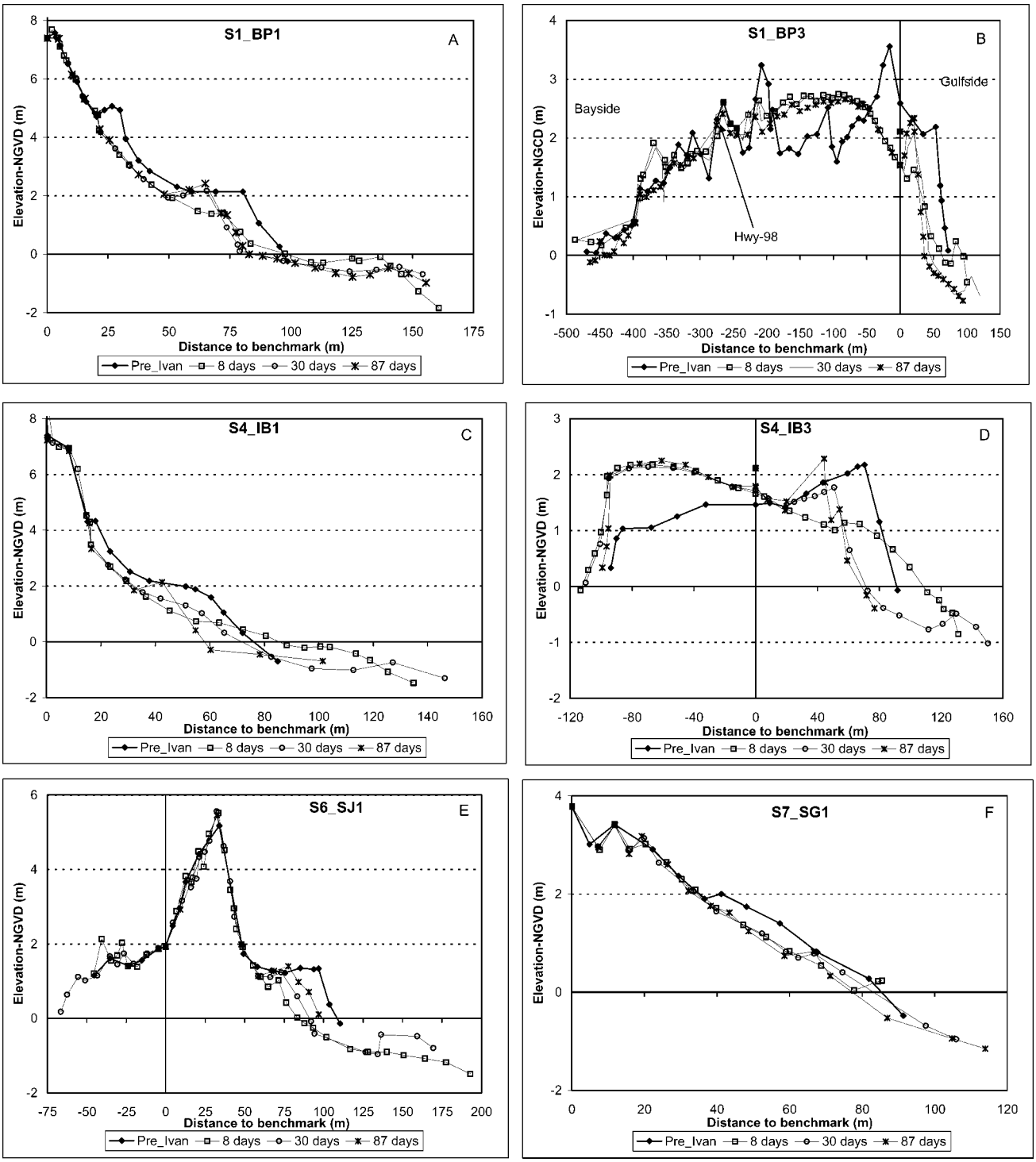

Figure 18. Short-term poststorm recovery. Note the rapid recovery of the berm and foreshore slope.

storm height of about 2 m above NGVD, whereas the recovered berm is located considerably landward (Figure 18). Both the pre- and recovered poststorm berm heights are slightly lower at S6_SJ as compared to the other sites, 1.4 m versus 2.0 m. This lower berm height may be attributed to the general north-south beach orientation at S6 versus the east-west orientation at the other sites. At S7_SG, the recovered poststorm berm is of a much lower elevation as compared to the

prestorm berm, 0.8 m versus 2.0 m. The reason for this lower berm-elevation recovery is not clear. The different prestorm beach-profile shape, which might be impacted by the earlier Hurricane Frances, may have some influence.

Except at S7_SG, the recovered poststorm berm crest is located approximately 15 m landward of the prestorm berm crest on the beaches that were not overwashed (Figure 18, S1_BP1, S4_IB1, and S6_SJ1). The reason for the similar distance between pre- and recovered poststorm berm crests over a large area, *i.e.,* the 15 m, is not clear. Figure 18 shows 3 examples from a total of 6 locations. Two other locations, S1_BP2 and S4_IB2, show a similar 15- m difference. The sixth location, S4_SJ2 (Figure 5), suffered significant structural damage. An emergency beach fill was placed 2 months after the impact. At the two overwashed sites, the recovered poststorm berm is located much further landward than the prestorm berm, approximately 40 m landward at S1_BP3 and 30 m landward at S4_IB3. This difference may be attributed to the more severe backbeach erosion at the overwashed sites.

At all the study sites, the recovered poststorm foreshore slope, from berm crest to low-tide line (roughly at NGVD 0), demonstrated an apparent tendency to approach the prestorm slope. This trend can be observed at both overwashed and nonoverwashed sites (Figure 18). This demonstrates the tendency of the foreshore, the most active portion of the beach in terms of sediment transport, to restore its prestorm equilibrium within a relatively short period of time. At most of the sites, the poststorm foreshore slope approached the prestorm slope within 30 days. The profiles at S4_IB took slightly longer. It has been well documented that storm beach demonstrates a much gentler slope (AUBREY and ROSS, 1975; BIRKEMEIER *et al.,* 1991; MORTON, 2002; MORTON and SALLENGER, 2003; SHEPARD, 1950; STONE *et al.,* 2004). This study shows that the gentle storm slope in the intertidal zone is rather temporary. The prestorm foreshore slope can be restored within 1 to several months.

Considerable elevation loss of up to 0.5 m was measured on the overwash platform, between Hwy 98 and the prestorm dune, at S1_BP3 during the 90-day period (Figure 18). Aeolian sand transport is likely responsible for this net loss. Active wind transport over the barren overwash platform was observed in the field. To prevent further sand loss over the overwash platform because of wind transport, sand fencing or artificial vegetation may be necessary.

CONCLUSIONS

Hurricane Ivan induced dramatic coastal changes in a large region along the northwest Florida Gulf coast, extending over 300 km east from the storm center. All four impact-scales as classified by SALLENGER (2000) occurred at a regional scale. The inundation and overwash regimes dominated the first 100 km east from the storm center. The collision regime with extensive dune scarping dominated from 100 to 150 km. The swash regime with severe backbeach erosion extends to over 300 km from the storm center. The intensity of storm impact as indicated by the elevation of the erosional limit decreased eastward from approximately 5 m at S1_BP to 2 m at S7_SG.

At sites that were not overwashed, severe backbeach/dune erosion occurred with a net loss of sand, up to 100 m^3/m, from the beach/dune system. At overwashed sites, a large amount of sand eroded from the backbeach and dune field deposited on the overwash platform. In other words, the swash and collision regimes resulted in significant net loss of sand from the backbeach/dune system. Although a tremendous amount of sand is redistributed during the overwash and inundation regimes, net loss or gain from the backbeach-dune and overwash-platform system is minimal.

Significant beach/dune erosion occurred considerably above the measured level of storm surge. Wave setup and swash run-up contributed significantly, on the order of 50% in the case of Ivan, to the maximum elevation of beach/dune erosion. Most of the existing empirical formulas overpredicted the values of wave setup and swash run-up. The steep foreshore slope and therefore large Iribarren number is attributable to the overprediction. The formulas that are independent of beach slope reproduced the measured values more closely.

Hurricane Ivan induced an apparent erosional surface on the backbeach and the impacted dune areas. This erosional surface extends eastward over 300 km from the storm center. A storm layer 10 to 50 cm thick was deposited on the erosional surface. The thickness of the subaerial storm deposits typically increases seaward from the dune scarp. Regionally, the thickness decreases eastward away from the storm center. In addition to storm intensity, the thickness of the storm deposits and its longshore and cross-shore trends are also influenced by factors such as sand supply from the dune field and beach width.

Short-term recovery occurred rather rapidly and was dominated by foreshore-slope restoration and berm growth. The steep prestorm foreshore slope was restored from the gentle storm-profile slope mostly within a month. The berm recovered to prestorm height within 90 days. However, the recovered berm was located approximately 15 m landward of the prestorm berm at sites that were not overwashed. At the overwashed sites S1_BP and S4_IB with severe backbeach erosion, the recovered berm was 40 and 30 m landward of the prestorm berm, respectively. Significant amount of sand, up to 0.5 thick in this case, can be lost from the barren overwash platform because of aeolian transport.

ACKNOWLEDGMENTS

The present study is supported by the University of South Florida and the National Science Foundation's Geography and Regional Science Program.

LITERATURE CITED

AUBREY, D.G. and ROSS, R.M., 1975. The quantitative description of beach cycles. *Marine Geology,* 69, 155–170.

BIRKEMEIER, W.A.; BICHNER, E.W.; SCARBOROUGH, B.L.; MCCONATHY, M.A., and EISER, W.C., 1991. Nearshore profile response caused by Hurricane Hugo. *Journal of Coastal Research,* Special Issue No. 8, pp. 113–127.

BUYNEVICH, I.V.; FITZGERALD, D.M., and VAN HETEREN, S., 2004. ?5

Sedimentary records of intense storms in Holocene barrier sequences, Maine, USA. *Marine Geology,* 210, 135–148.

COLEMAN, C., 1978. The Stranded Bar: A Study of Bar Formation during Storm Surges at Carrabelle Beach, Florida. Tallahassee, Florida: Florida State University, Master's thesis, 156p.

DINGLER, J.R. and REISS, T.E., 1995. Beach erosion on Trinity Island, Louisiana caused by Hurricane Andrew. *Journal of Coastal Research,* Special Issue No. 21, pp. 254–264.

DOUGHERTY, A.J.; FITZGERALD, D.M., and BUYNEVICH, I.V., 2004. Evidence for storm-dominated early progradation of Castle Neck barrier, Massachusetts, USA. *Marine Geology,* 210, 123–134.

FINKL, C.W. and PILKEY, O.H. (eds.), 1991. Impacts of Hurricane Higo: September 10–22 1989. *Journal of Coastal Research,* Special Issue No. 8, 356p.

FITZGERALD, D.M.; VAN HETEREN, S., and MONTELLO, T.M., 1994. Shoreline processes and damage resulting from the Halloween Eve storm of 1991 along the North and South shores of Massachusetts Bay, U.S.A. *Journal of Coastal Research,* 10, 113–132.

GUZA, R.T. and THORNTON, E.B., 1980. Local and shoaled comparisons of sea surface elevations, pressures and velocities. *Journal of Geophysical Research,* 85(C3), 1524–1530.

GUZA, R.T. and THORNTON, E.B., 1981. Wave set-up on a natural beach. *Journal of Geophysical Research,* 86(C5), 4133–4137.

GUZA, R.T. and THORNTON, E.B., 1982. Swash oscillations on a natural beach. *Journal of Geophysical Research,* 87(C1), 483–491.

HOLMAN, R.A., 1986. Extreme value statistics for wave run-up on a natural beach. *Coastal Engineering,* 9, 527–544.

KEEN, T. R. and STONE, G.W., 2000. Anomalous response of beaches to hurricane waves in a low-energy environment, northeast Gulf of Mexico, U.S.A. *Journal of Coastal Research,* 16, 1100–1110.

LEATHERMAN, S.P.; WILLIAMS, A.T., and FISHER, J.S., 1977. Overwash sedimentation associated with a large scale northeaster. *Marine Geology,* 24, 109–121.

LEATHERMAN, S.P. and ZAREMBA, R.E., 1987. Overwash and aeolian processes on a U.S. northeast barrier. *Sedimentary Geology,* 52, 183–206.

MORANG, A., 1992. Inlet migration and hydraulic processes at East Pass, Florida. *Journal of Coastal Research,* 8, 457–481.

MORTON, R.A., 2002. Factors controlling storm impacts on coastal barriers and beaches—a preliminary basis for real-time forecasting. *Journal of Coastal Research,* 18, 486–501.

MORTON, R.A. and SALLENGER, A.H., JR., 2003. Morphological impacts of extreme storms on sandy beaches and barriers. *Journal of Coastal Research,* 19, 560–574.

RUGGIERO, P.; KOMAR, P.D.; MCDOUGAL, W.C.; MARRA, J.J., and BEACH, R.A., 2001. Wave runup, extreme wave levels and the erosion of properties backing beaches. *Journal of Coastal Research,* 17, 407–419.

SALLENGER, A.H., 2000. Storm impact scale for barrier islands. *Journal of Coastal Research,* 16, 890–895.

SALLENGER, A.H. and HOLMAN, R.A., 1985. Wave energy saturation on a natural beach of variable slope. *Journal of Geophysical Research,* 90(C6), 11939–11944.

SCHWARTZ, R.K., 1975. Nature and Genesis of Some Storm Washover Deposits. CERC Technical Memo 61, Army Corps of Engineers, 69p.

SCHWARTZ, R.K., 1982. Bedform and stratification characteristics of some modern small-scale washover sand bodies. *Sedimentology,* 29, 8.5–849.

SEDGWICK, P.E. and DAVIS, R.A., JR., 2003. Stratigraphy of washover deposits in Florida: implications for recognition in the stratigraphic record. *Marine Geology,* 200, 31–48.

SHEPARD, F.P., 1950. Beach cycles in Southern California. Technical Memo No. 20, U.S. Army Corps of Engineers, Beach Erosion Board, 26p.

STAPOR, F.W., 1973. History and sand budgets of the barrier island system in the Panama City, Florida region. *Marine Geology,* 14, 277–286.

STONE, G.W., 1991. Differential Sediment Supply and the Cellular Nature of Longshore Sediment Transport along Coastal Northwest Florida and Southeast Alabama since the Late Holocene. College Park, Maryland: University of Maryland, Ph.D. dissertation, 376p.

STONE, G.W. and FINKL, C.W. (eds.), 1995. Impacts of Hurricane Andrew on the coastal zones of Florida and Louisiana: 22–26 August 1992. *Journal of Coastal Research,* Special Issue No. 21, 364p.

STONE, G.W. and ORFORD, J.D., 2004. Storm and their significance in coastal morpho-sedimentary dynamics. *Marine Geology,* 210, 1–5.

STONE, G.W. and WANG P., 1999. The importance of cyclogenesis on the short-term evolution of Gulf coast barriers. *Transactions, Gulf Coast Association of Geological Society,* XLIX, 478–486.

STONE, G.W.; LIU, B.; PEPPER, D.A., and WANG P., 2004. The importance of extratropical and tropical cyclones on the short-term evolution of barrier islands along the northern Gulf of Mexico, USA. *Marine Geology,* 210, 63–78.

STONE, G.W.; WANG, P.; PEPPER, D.A.; GRYMES, J.W.; BOBERTS, H.H.; ZHANG, X.P.; HSU, S.A., and HUH, O.K., 1999. Researchers begin to unravel the significane of hurricanes of the northern Gulf of Mexico. *EOS Transactions of the American Geophysical Union,* 80, 301–305.

TEDESCO, P.L.; WANLESS, H.R.; SCUSA, L.A.; RISI, J.A., and GELSANLITER, S., 1995. Impact of Hurricane Andrew on south Florida's sandy coastlines. *Journal of Coastal Research,* Special Issue No. 21, pp. 59–82.

UNITED STATES DEPARTMENT OF AGRICULTURE: SOIL CONSERVATION SERVICE (USDA-SCS), 1984. Soil Survey of Bay County, Florida. Washington, DC: U.S. Government Printing Office.

USDA-SCS, 1989. Soil Survey of Walton County, Florida. Washington, DC: U.S. Government Printing Office.

WANG, P. and DAVIS, R.A., JR., 1998. A beach profile model for a barred coast—case study from Sand Key, west-central Florida. *Journal of Coastal Research,* 14(3), 981–991.

WELLS, J.T. and MCNINCH, J., 1991. Beach scraping in North Carolina with special reference to its effectiveness during Hurricane Hugo. *Journal of Coastal Research,* Special Issue No. 8, pp. 249–262.